Response to Anonymous Referee #1

We thank the reviewer for the constructive suggestions/comments. Below we provide a point-by-point response to individual comment (Reviewer comments and suggestions are in italics, responses and revisions are in plain font; revised parts in responses are marked with red color; page numbers refer to the modified AMTD version).

Comments and suggestions:

Overall Comments. Heterogeneous and multiphase reactions in the atmosphere can affect the formation and transformation of pollutants and determine the composition of gases and aerosol. Kinetic study is used to evaluate the impact of heterogeneous and multiphase reactions on the atmosphere environment. This manuscript developed a method to measure gas uptake coefficients, explained the principle of the method in detail and evaluated the measurement results. This study has made a good attempt; however, some concerns still remain. So, I think it needs some revisions before publication.

Responses and Revisions:

Thanks for the positive comments and feedback from the reviewer.

Comments and suggestions:

Specific Comments. The introduction procedure of reactant gas and sample may not be suitable. When the lid is opened to place the sample, the reactor is filled with high concentration of reactant gas. At this time, the sample has been in contact with these high concentration reactant gases for a period of time during the placement, resulting in the occupation of its surface-active sites and thus affecting the measurement of initial uptake coefficients. This method may be effective for the measurement of steady-state uptake coefficient, however, there are very few heterogeneous reactions that can take place in a steady-state. So, its application may be limited.

Responses and Revisions:

Thanks for the comments.

In order to evaluate the degree of saturation on sample surfaces during our sample placement operation period (i.e., 0 - 5 min), we estimated the sample surface coverage (in percentage) corresponding to the first 5-min of potential uptake assuming: (1) one molecule of the gas reactants

(O_3 and SO_2) adsorbed on sample surfaces would occupy/consume an area equaling to the cross-section area of the spherical gas molecule; (2) the gas molecules could diffuse into the bulk of the samples and adsorption inside the bulk (i.e., on pore surfaces) occurred, but the pore diffusion rate was not considered as a limiting factor; (3) surface saturation was defined as one monolayer of the gas molecules formed on the whole surface of samples. Then, the number of molecules needed to form such a monolayer, N_{total}, can be calculated as:

$$N_{total} = \frac{S_{BET}}{S_M} = \frac{4S_{BET}}{\pi d^2} \quad \text{(ER1)}$$

where S_M and d are the cross-section area and diameter of the reactant gas molecule (O_3 or SO_2), respectively. S_{BET} is the specific surface area of the used samples.

The number of molecules adsorbed on sample surfaces after a time span of t, $N(t)$, is given by:

$$N(t) = \frac{v}{4}\gamma_{BET}S_{BET}C_{ref}t \quad \text{(ER2)}$$

where v is the mean molecular speed and γ_{BET} is the uptake coefficient derived based on S_{BET}. C_{ref} is the measured gas concentration at the outlet of the blank chamber. Since we didn't measure the gas concentration above the sample during our sample placement period, we took C_{ref} as an upper limit and the real concentration should be lower. Finally, the sample surface coverage θ can be estimated as:

$$\theta = \frac{N(t)}{N_{total}} \quad \text{(ER3)}$$

Table R1. Parameters and results for sample surface coverage estimation

Uptake scenarios	γ_{BET}[a]	C_{ref} (molecules m^{-3})	S_{BET} (m^2)	v[b] (m s^{-1})	d[c] (nm)	S_M (m^2)	t (s)	$N(t)$ (molecules)	N_{total} (molecules)	θ (%)
O_3 + SiO_2	2.00E-07	9.31E+17	11.0	361	0.5	1.96E-19	300	5.54E+16	5.60E+19	0.1
O_3 + Fe_2O_3	1.79E-06	2.66E+18	7.2	361	0.5	1.96E-19	300	9.27E+17	3.67E+19	2.53
SO_2 + TiO_2	5.22E-07	3.58E+18	20.5	313	0.28	6.15E-20	300	9.00E+17	3.33E+20	0.3
SO_2 + Fe_2O_3	1.29E-06	2.65E+18	8.0	313	0.28	6.15E-20	300	6.44E+17	1.30E+20	0.5

a: Given that the measured gas centration at the sample chamber outlet (i.e., C_{out}) displays an increasing trend for the uptake scenario O_3+SiO_2, its γ_{BET} was recalculated by using a C_{out} corresponding to the uptake time of 1 min (i.e., the time point of 1 min during the sample placement operation period) and assuming that this C_{out} generally represents the

average among the first 5-min of uptake. The C_{out} at uptake time of 1 min was obtained by logarithmically fitting and extrapolating the C_{out} time series between 6 -10 min (i.e., the time period we used for data analysis in our manuscript). For the other scenarios, the γ_{BET} were directly taken from our measurement results (i.e., the values shown in Fig. 7 in the revised manuscript), as their C_{out} are fairly constant during the measurements. The measured time series of C_{out} for all the uptake scenarios can be found below (Fig. R1). **b**: The mean molecular speed values correspond to our experimental conditions of 296 K and 1 atm. **c**: The molecular diameter of O_3 is referred to (Zhou et al., 2013) and the one of SO_2 to (Dou et al., 2020).

Table R1 shows the related parameters adopted for θ calculation and the results. The low θ values for all the uptake scenarios indicate that the sample surfaces didn't undergo a significant saturation process during our sample placement operation periods. Note that the results we obtained only help to provide a qualitative understanding of the overall uptake process. Normally the uptake coefficients derived based on the specific surface area of samples (γ_{BET}) represent the lower limit of a potential uptake coefficient range, this may explain the very low θ values here we have. Early studies (Kalberer et al., 1999) have suggested that initial uptake (in a time scale of seconds) can also be irrelevant for atmospheric conditions. Thus, the time span (in minutes, but can be extended to hours) covered by our system may have advantages in determining uptake coefficients of more atmospheric relevance.

Moreover, in order to measure uptake coefficients at the initial stage of uptake, a modification may be needed for our chamber system. One easy solution would be adding a cover (chemically inert) on the sample-holding petri dish, which can be easily removed inside the chamber but without opening it. Then, a new introduction procedure can be designed as: (1) put the covered sample-holding petri dish onto the chamber bottom; (2) close the chamber lid; (3) feed gas reactant into the chamber until its concentration reaches a steady state; (4) remove the petri dish cover inside the chamber to allow gas uptake on samples. The use of the cover could avoid uptake of gas reactants on samples before the steady-state concentration is reached. We suggest that future chamber applications could consider to use this way for gas kinetic studies.

We have added these discussions in the revised manuscript (page 11, line 19-28), as follows:

"3.1.1 Chamber equilibrium time

…For our uptake experiments, the freshly prepared samples were exposed to the gas reactants for 10 min and only uptake data in the second half of the exposure period (i.e., 6 - 10 min) were used

for γ calculation. In order to measure γ at the initial stage of uptake, a modification may be needed for our chamber system. One easy solution would be adding a cover (chemically inert) on the sample-holding petri dish, which can be easily removed inside the chamber but without opening it. Then, a new introduction procedure can be designed as: (1) put the covered sample-holding petri dish onto the chamber bottom; (2) close the chamber lid; (3) feed gas reactant into the chamber until its concentration reaches a steady state; (4) remove the petri dish cover inside the chamber to allow gas uptake on samples. The use of the cover could avoid uptake of gas reactants on samples before the steady-state concentration is reached in the chamber. We suggest that future chamber applications could consider to use this way for gas kinetic studies."

Comments and suggestions:

Specific Comments. The influence of gas diffusion in the reactor on the kinetics was not sufficiently evaluated. Due to the defects of the sample placement mentioned above, the selection of exposure time seems not rigorous. In addition, the effect of the types of samples and reaction gases on the time to reach steady-state is not known. The wall loss of reaction gas under different humidity conditions also needs to be characterized.

Responses and Revisions:

Thanks for the comments.

The influence of gas diffusion inside our chamber on the measured uptake coefficient is mainly discussed in page 5 from line 6 to line 28, where we introduce a method to measure the transport-limited deposition velocity V_t. V_t specifically reflects the gas diffusion conditions inside the chamber. For our case, gas diffusion includes turbulent diffusion and laminar/molecular diffusion. The former is produced and regulated by the mixing fan and the latter occurs in the quasi-laminar layer just above the sample surface. Assuming the method we used for V_t determination can generally have the same gas diffusion conditions as in the uptake experiment, the determined V_t takes all the gas-diffusion-related uptake kinetics into account for later on uptake coefficient derivation. Therefore, the influence of gas diffusion on the kinetics is represented by V_t.

In this work, the selection of exposure time is based on the chamber equilibrium time determined via chamber characterization experiments. This chamber equilibrium time only accounts for the gas dilution (due to the chamber opening operation, the lab air would dilute the gas reactant

concentration inside the chamber) and the chamber wall loss effects. The selection of our data time period (6 - 10 min) is based on an assumption that the equilibrium time (5 min, see Fig. 3) of the blank chamber is the same as that of the sample chamber. Only in this case can C_{ref} be used for uptake coefficients calculation.

As the reviewer mentioned, the effect of the types of samples and reaction gases on the time to reach steady state is not specifically characterized in this study. Since here we only did the uptake experiments with a timescale of 10 min, the relatively short time didn't allow us to see the whole picture of the evolvement of uptake as a function of time. Figure R1 shows the time series of the gas reactants concentrations from typical uptake experiments in this study. For the first uptake scenario (O_3 + SiO_2), the measured concentrations at the sample chamber outlet (i.e., C_{out}) show a gradually increasing trend during our experiment period (6 – 10 min), indicating that the uptake didn't reach a steady state. For the other scenarios, however, their C_{out} keep fairly constant, characteristic of steady-state uptake. As reported in previous studies (Bulanin et al., 1994; Hanisch and Crowley, 2003; Michel et al., 2003; Usher et al., 2002; Adams et al., 2005), the different uptake behaviors can be due to their distinct uptake mechanisms. Note that, in this study, our focus is not exploring the changing behavior of uptake coefficients as a function of time for different types of samples and gas reactants, but rather to examine and show the validity of the chamber technique (and the adopted calculation method for uptake coefficients derivation) for kinetic studies. Thus, we used the average C_{out} (6 – 10 min) for uptake coefficients calculation and compared our results with previous studies with similar uptake timescales (see Fig. 7). Our chamber system could still allow to investigate gas uptake kinetics with extended time scales in future studies.

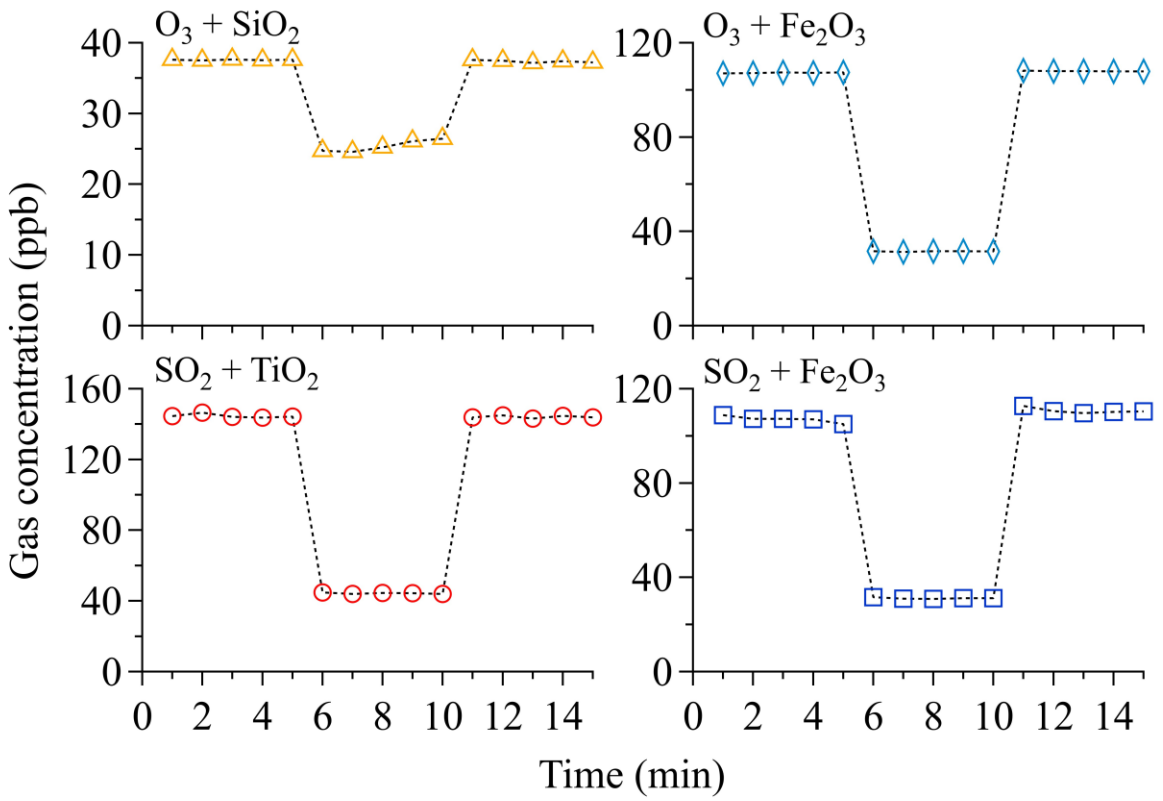

Figure R1. Time series of gas reactants (O_3 and SO_2) concentrations. For each scenario, the results from one typical uptake experiment is shown. The data in the time period of 6 – 10 min denote gas concentrations at the sample chamber outlet (C_{out}) and in the other periods represent gas concentrations at the blank chamber outlet (C_{ref}).

Regarding the wall loss of reaction gas under different humidity conditions, all our uptake experiments were performed with pre-humidified (50 ± 1% relative humidity (RH)) zero air. This means that the RH inside the chamber was around 50% for all uptake experiments with solid samples. For the uptake experiments with deliquescent KI grains and saturated KI solutions (see Sect. 3.1.3), the RH inside the chamber was 73% and 92%, respectively. Actually, the wall loss of reaction gas under these different RH conditions had been characterized before each uptake experiment and corrected for the uptake coefficient calculation. To make this information more clear, we have added some explanations in the revised manuscript (page 4, line 1-6), as shown below:

"…where C_{ref} (in molecules m^{-3}) is the gas reactant concentration measured at the outlet of a blank chamber prior to the uptake experiment. Since our chamber system had a dynamic flow-through

feature, a constant rate of wall loss (once existed) was observed, i.e., the ratio of C_{ref} to C_{in} showed a fixed value during our uptake experiments (see Fig. 3). Thus, using C_{ref} (instead of C_{in}) for flux calculation already accounted for gas losses on chamber walls. Before each gas uptake experiment, C_{ref} was determined mimicking the chamber conditions (i.e., gas flow rate, gas mixing state, temperature, pressure and RH, and the speed of the mixing fan) of the following uptake experiments."

Comments and suggestions:

Specific Comments. The derivation of the formula should give the dimension or unit like in formula 6.

Responses and Revisions:

Thanks for the suggestion.

The related modifications have been made in the revised manuscript (page 3 line 19 to page 5 line 28), as shown below:

"2.1.1 Uptake coefficient determination

Dynamic flow-through chambers had been widely adopted in previous studies to measure trace gas exchange rates between the atmosphere and biosphere such as vegetation and soils (Pumpanen et al., 2001; Gut et al., 2002; Pape et al., 2009; Su et al., 2011; Breuninger et al., 2012; Oswald et al., 2013; Cowan et al., 2014; Almand-Hunter et al., 2015; Plake et al., 2015; Weber et al., 2015; Sun et al., 2016; Meusel et al., 2016; Meusel et al., 2018; Wu et al., 2019). Similarly, in our chamber the flux J (in molecules s^{-1}) of a gas reactant can be calculated from the mass balance by

$$J = Q \times (C_{in} - C_{out}) \quad (1)$$

where Q is the chamber flow rate (in m^3 s^{-1}), C_{in} is the supplied trace gas concentration at the chamber inlet (in molecules m^{-3}), C_{out} is the trace gas concentration at the outlet of the chamber containing a sample (in molecules m^{-3}). Note that in Eq. (1) the difference between C_{in} and C_{out} can be arised not only from gas uptake on the sample but also from its losses on the chamber wall. Here, as we only focus on gas uptake on samples, the chamber wall loss effect should be corrected beforehand. Thus, the flux J_{sam} caused solely by gas reactant at the sample surface is calculated as

$$J_{sam} = Q \times (C_{ref} - C_{out}) \quad (2)$$

where C_{ref} (in molecules m^{-3}) is the gas reactant concentration measured at the outlet of a blank chamber prior to the uptake experiment. Since our chamber system had a dynamic flow-through feature, a constant rate of wall loss (once existed) was observed, i.e., the ratio of C_{ref} to C_{in} showed a fixed value during our uptake experiments (see Fig. 3). Thus, using C_{ref} (instead of C_{in}) for flux calculation already accounted for gas losses on chamber walls. Before each gas uptake experiment, C_{ref} was determined mimicking the chamber conditions (i.e., gas flow rate, gas mixing state, temperature, pressure and RH, and the speed of the mixing fan) of the following uptake experiments.

Assuming a well-mixed and steady-state condition in the chamber, the deposition velocity V_d (in $m\ s^{-1}$) at the chamber outlet can be derived as (Seinfeld and Pandis, 2016):

$$V_d = \frac{J_{sam}}{C_{out} \times A} \quad (3)$$

where A is the cross-sectional area at the chamber outlet (in m^2), which equals the surface area of the chamber bottom.

The deposition velocity can be used to calculate the surface uptake/reaction kinetics. In analogy to electrical resistances under both ambient (Seinfeld and Pandis, 2016) and chamber-modified conditions (Pape et al., 2009), the uptake process can be decomposed into two processes: transport to the surface and uptake on the surface. A simplified two-resistor model proposed by Canoruiz et al., (1993) is therefore used:

$$\frac{1}{V_d} = R_t + R_s = \left(\frac{1}{V_t} + \frac{4}{\gamma_{obs} \times \omega}\right) \quad (4)$$

where R_t is the transport resistance (in $s\ m^{-1}$), which equals the reciprocal of the transport-limited deposition velocity V_t (in $m\ s^{-1}$); R_s is the surface uptake resistance (in $s\ m^{-1}$), which is determined by the observed uptake coefficient γ_{obs} and the mean molecular speed ω of the gas reactant (in $m\ s^{-1}$). Comparison between this two-resistor model and the resistance model (for dry deposition) proposed by Seinfeld and Pandis (2016) reveals that the transport resistance R_t can be viewed as the sum of the aerodynamic resistance R_a and the quasi-laminar layer resistance R_b. Thus, R_t (or V_t) is dependent on the flow/mixing conditions in the chamber (accounting for R_a and R_b) as well as the molecular diffusivity of the gas reactant itself (accounting for R_b).

Based on Eqn. (4), an expression for the observed/measured uptake coefficient γ_{obs} can be given as:

$$\gamma_{obs} = \left(\frac{\omega}{4}\left(\frac{1}{V_d} - \frac{1}{V_t}\right)\right)^{-1} \quad (5)$$

After accounting for the sample mass m_s, we can finally get the mass-independent uptake coefficient γ_{BET}:

$$\gamma_{BET} = \gamma_{obs} \times \left(\frac{A}{A_{ss}}\right) = \gamma_{obs} \times \left(\frac{A}{m_s \times S_{BET}}\right) \quad (6)$$

where A_{ss} is the sample specific surface area (in m^2), which equals the sample mass m_s (in g) times the sample specific BET surface area S_{BET} (in m^2 g^{-1}). One should keep in mind that for liquid samples in a petri dish, A_{ss} is equivalent to the geometric surface area of the petri dish. Moreover, adopting A_{ss} for γ_{BET} calculation only holds when the whole sample coating contributes to uptake of the gas reactant within the experiment period. Using the method described in our previous study (Li et al., 2019) a maximum diffusion time of ~ 5 min is estimated for O_3/SO_2 penetrating through our solid samples, which is comparable to our uptake experiment time scale (i.e., reaction time of ~ 5 - 10 min).

V_d can be calculated through Eqn. (3) based on chamber flux measurements. Actually, V_t can be viewed as a special situation when $R_s << R_t$ (i.e., when γ is in the range of 10^{-2} - 1, $4/(\gamma \times \omega)$ is in the range of 10^{-4} – 10^{-2} s cm^{-1}, which is two to four orders of magnitudes smaller than R_t, see Sect. 3.1.3. Note that at our experimental temperature of 23 °C, ω_{SO2} = 313 m s^{-1} and ω_{O3} = 361 m s^{-1}). Therefore, V_t can be obtained experimentally by finding a specific trace gas species with a γ on the order of 10^{-2} to 1. Saturated potassium iodide (KI) solutions and solid KI coatings have been demonstrated to be a perfect sink for O_3 with a γ up to 10^{-2} (Galbally and Roy, 1980; Parmar and Grosjean, 1990; Rouvière et al., 2010) and have been used to obtain V_t (Morrison and Nazaroff, 2000; Coleman et al., 2008; Pape et al., 2009). Note that the determined V_t depends on the chamber setup and experimental conditions (i.e., gas flow rate, gas mixing state, temperature, pressure and RH, and the speed of the mixing fan). Because physical properties of samples can potentially influence R_b (e.g., the surface roughness of a sample can affect the thickness of the quasi-laminar layer above it) and hence R_t, the KI samples should also have the same or similar phase state and surface morphology as those of the investigated samples. Thus, in this study, V_t was determined by measuring O_3 uptake on different types of KI substrates (i.e., saturated KI solutions, KI

films/grains held in a petri dish, see Sect. 3.1.3), to check the effects of their phase state and surface morphology on V_t. On the other hand, when R_b is the limiting step for V_t, the determined V_t based on O_3 uptake on KI cannot be directly used for other gas reactants. A correction is therefore necessary (Goldan et al., 1988):

$$V_{t,i} = V_{t,O_3} \times \sqrt{\frac{M_{O_3}}{M_i}} \quad (7)$$

where $V_{t,i}$ is the transport-limited deposition velocity of gas reactant i (in m s^{-1}), $V_{t,O3}$ is the observed transport-limited deposition velocity of O_3 (in m s^{-1}), and M_i and M_{O3} are the molar mass of i and O_3 (in g mol^{-1}), respectively. Notably, turbulent diffusion is not affected by molecular weight, hence the V_t correction becomes exaggerated for cases where $R_a >> R_b$. We estimated R_a and R_b according to our chamber configuration and experimental conditions. Details about comparisons between R_a and R_b can be found in the Supplement. These results show that R_a is several times larger than R_b when solid oxide samples are used for uptake experiments. Herein, V_t measured by O_3 uptake on KI can be used as a close approximation of V_t in uptake experiments of other reactive gases."

References

Adams, J. W., Rodriguez, D., and Cox, R. A.: The uptake of SO₂ on Saharan dust: a flow tube study, Atmos. Chem. Phys., 5, 2679-2689, 10.5194/acp-5-2679-2005, 2005.

Almand-Hunter, B. B., Walker, J. T., Masson, N. P., Hafford, L., and Hannigan, M. P.: Development and validation of inexpensive, automated, dynamic flux chambers, Atmospheric Measurement Techniques, 8, 267-280, 2015.

Breuninger, C., Oswald, R., Kesselmeier, J., and Meixner, F. X.: The dynamic chamber method: trace gas exchange fluxes (NO, NO₂, O₃) between plants and the atmosphere in the laboratory and in the field, Atmos. Meas. Tech., 5, 955-989, 10.5194/amt-5-955-2012, 2012.

Bulanin, K. M., Alexeev, A. V., Bystrov, D. S., Lavalley, J. C., and Tsyganenko, A. A.: IR Study of Ozone Adsorption on SiO2, The Journal of Physical Chemistry, 98, 5100-5103, 10.1021/j100070a026, 1994.

Canoruiz, J. A., Kong, D., Balas, R. B., and Nazaroff, W. W.: Removal of Reactive Gases at Indoor Surfaces - Combining Mass-Transport and Surface Kinetics, Atmospheric Environment Part a-General Topics, 27, 2039-2050, 1993.

Coleman, B. K., Destaillats, H., Hodgson, A. T., and Nazaroff, W. W.: Ozone consumption and volatile byproduct formation from surface reactions with aircraft cabin materials and clothing fabrics, Atmospheric Environment, 42, 642-654, 2008.

Cowan, N. J., Famulari, D., Levy, P. E., Anderson, M., Reay, D. S., and Skiba, U. M.: Investigating uptake of N₂O in agricultural soils using a high-precision dynamic chamber method, Atmos. Meas. Tech., 7, 4455-4462, 10.5194/amt-7-4455-2014, 2014.

Dou, J., Zhao, Y., Duan, X., Chai, H., Li, L., and Yu, J.: Desulfurization Performance and Kinetics of Potassium Hydroxide-Impregnated Char Sorbents for SO2 Removal from Simulated Flue Gas, ACS Omega, 5, 19194-19201, 10.1021/acsomega.0c02624, 2020.

Galbally, I. E., and Roy, C. R.: Destruction of ozone at the earth's surface, Quarterly Journal of the Royal Meteorological Society, 106, 599-620, 10.1002/qj.49710644915, 1980.

Goldan, P. D., Fall, R., Kuster, W. C., and Fehsenfeld, F. C.: Uptake of COS by growing vegetation: A major tropospheric sink, Journal of Geophysical Research: Atmospheres, 93, 14186-14192, 10.1029/JD093iD11p14186, 1988.
Gut, A., Scheibe, M., Rottenberger, S., Rummel, U., Welling, M., Ammann, C., Kirkman, G. A., Kuhn, U., Meixner, F. X., Kesselmeier, J., Lehmann, B. E., Schmidt, W., Müller, E., and Piedade, M. T. F.: Exchange fluxes of NO2 and O3 at soil and leaf surfaces in an Amazonian rain forest, Journal of Geophysical Research: Atmospheres, 107, LBA 27-21-LBA 27-15, 10.1029/2001JD000654, 2002.
Hanisch, F., and Crowley, J. N.: Ozone decomposition on Saharan dust: an experimental investigation, Atmos. Chem. Phys., 3, 119-130, 10.5194/acp-3-119-2003, 2003.
Kalberer, M., Ammann, M., Arens, F., Gäggeler, H. W., and Baltensperger, U.: Heterogeneous formation of nitrous acid (HONO) on soot aerosol particles, Journal of Geophysical Research: Atmospheres, 104, 13825-13832, https://doi.org/10.1029/1999JD900141, 1999.
Li, G., Cheng, Y., Kuhn, U., Xu, R., Yang, Y., Meusel, H., Wang, Z., Ma, N., Wu, Y., Li, M., Williams, J., Hoffmann, T., Ammann, M., Pöschl, U., Shao, M., and Su, H.: Physicochemical uptake and release of volatile organic compounds by soil in coated-wall flow tube experiments with ambient air, Atmos. Chem. Phys., 19, 2209-2232, 10.5194/acp-19-2209-2019, 2019.
Meusel, H., Kuhn, U., Reiffs, A., Mallik, C., Harder, H., Martinez, M., Schuladen, J., Bohn, B., Parchatka, U., Crowley, J. N., Fischer, H., Tomsche, L., Novelli, A., Hoffmann, T., Janssen, R. H. H., Hartogensis, O., Pikridas, M., Vrekoussis, M., Bourtsoukidis, E., Weber, B., Lelieveld, J., Williams, J., Pöschl, U., Cheng, Y., and Su, H.: Daytime formation of nitrous acid at a coastal remote site in Cyprus indicating a common ground source of atmospheric HONO and NO, Atmos. Chem. Phys., 16, 14475-14493, 10.5194/acp-16-14475-2016, 2016.
Meusel, H., Tamm, A., Kuhn, U., Wu, D., Leifke, A. L., Fiedler, S., Ruckteschler, N., Yordanova, P., Lang-Yona, N., Pöhlker, M., Lelieveld, J., Hoffmann, T., Pöschl, U., Su, H., Weber, B., and Cheng, Y.: Emission of nitrous acid from soil and biological soil crusts represents an important source of HONO in the remote atmosphere in Cyprus, Atmos. Chem. Phys., 18, 799-813, 10.5194/acp-18-799-2018, 2018.
Michel, A. E., Usher, C. R., and Grassian, V. H.: Reactive uptake of ozone on mineral oxides and mineral dusts, Atmospheric Environment, 37, 3201-3211, http://dx.doi.org/10.1016/S1352-2310(03)00319-4, 2003.
Morrison, G. C., and Nazaroff, W. W.: The rate of ozone uptake on carpets: Experimental studies, Environmental Science & Technology, 34, 4963-4968, 2000.
Oswald, R., Behrendt, T., Ermel, M., Wu, D., Su, H., Cheng, Y., Breuninger, C., Moravek, A., Mougin, E., Delon, C., Loubet, B., Pommerening-Röser, A., Sörgel, M., Pöschl, U., Hoffmann, T., Andreae, M. O., Meixner, F. X., and Trebs, I.: HONO Emissions from Soil Bacteria as a Major Source of Atmospheric Reactive Nitrogen, Science, 341, 1233-1235, 10.1126/science.1242266, 2013.
Pape, L., Ammann, C., Nyfeler-Brunner, A., Spirig, C., Hens, K., and Meixner, F. X.: An automated dynamic chamber system for surface exchange measurement of non-reactive and reactive trace gases of grassland ecosystems, Biogeosciences, 6, 405-429, 10.5194/bg-6-405-2009, 2009.
Parmar, S. S., and Grosjean, D.: Laboratory Tests of Ki and Alkaline Annular Denuders, Atmospheric Environment Part a-General Topics, 24, 2695-2698, 1990.
Plake, D., Stella, P., Moravek, A., Mayer, J. C., Ammann, C., Held, A., and Trebs, I.: Comparison of ozone deposition measured with the dynamic chamber and the eddy covariance method, Agricultural and Forest Meteorology, 206, 97-112, http://dx.doi.org/10.1016/j.agrformet.2015.02.014, 2015.
Pumpanen, J., Ilvesniemi, H., Keronen, P., Nissinen, A., Pohja, T., Vesala, T., and Hari, P.: An open chamber system for measuring soil surface CO2 efflux: Analysis of error sources related to the chamber system, Journal of Geophysical Research: Atmospheres, 106, 7985-7992, 10.1029/2000JD900715, 2001.
Rouvière, A., Sosedova, Y., and Ammann, M.: Uptake of Ozone to Deliquesced KI and Mixed KI/NaCl Aerosol Particles, The Journal of Physical Chemistry A, 114, 7085-7093, 10.1021/jp103257d, 2010.
Seinfeld, J. H., and Pandis, S. N.: Dry Deposition, in: Atmospheric Chemistry and Physics: from Air Pollution to Climate Change, 3rd ed., John Wiley & Sons, Inc., Hoboken, New Jersey, 2016.
Su, H., Cheng, Y., Oswald, R., Behrendt, T., Trebs, I., Meixner, F. X., Andreae, M. O., Cheng, P., Zhang, Y., and Pöschl, U.: Soil Nitrite as a Source of Atmospheric HONO and OH Radicals, Science, 333, 1616-1618, 10.1126/science.1207687, 2011.
Sun, S., Moravek, A., von der Heyden, L., Held, A., Sorgel, M., and Kesselmeier, J.: Twin-cuvette measurement technique for investigation of dry deposition of O-3 and PAN to plant leaves under controlled humidity conditions, Atmospheric Measurement Techniques, 9, 599-617, 2016.

Usher, C. R., Al-Hosney, H., Carlos-Cuellar, S., and Grassian, V. H.: A laboratory study of the heterogeneous uptake and oxidation of sulfur dioxide on mineral dust particles, Journal of Geophysical Research: Atmospheres, 107, ACH 16-11-ACH 16-19, 10.1029/2002JD002051, 2002.
Weber, B., Wu, D., Tamm, A., Ruckteschler, N., Rodríguez-Caballero, E., Steinkamp, J., Meusel, H., Elbert, W., Behrendt, T., Sörgel, M., Cheng, Y., Crutzen, P. J., Su, H., and Pöschl, U.: Biological soil crusts accelerate the nitrogen cycle through large NO and HONO emissions in drylands, Proceedings of the National Academy of Sciences, 112, 15384-15389, 10.1073/pnas.1515818112, 2015.
Wu, D., Horn, M. A., Behrendt, T., Müller, S., Li, J., Cole, J. A., Xie, B., Ju, X., Li, G., Ermel, M., Oswald, R., Fröhlich-Nowoisky, J., Hoor, P., Hu, C., Liu, M., Andreae, M. O., Pöschl, U., Cheng, Y., Su, H., Trebs, I., Weber, B., and Sörgel, M.: Soil HONO emissions at high moisture content are driven by microbial nitrate reduction to nitrite: tackling the HONO puzzle, The ISME Journal, 13, 1688-1699, 10.1038/s41396-019-0379-y, 2019.
Zhou, S., Shiraiwa, M., McWhinney, R. D., Pöschl, U., and Abbatt, J. P. D.: Kinetic limitations in gas-particle reactions arising from slow diffusion in secondary organic aerosol, Faraday Discussions, 165, 391-406, 10.1039/C3FD00030C, 2013.

Response to Anonymous Referee #2

We thank the reviewer for the constructive suggestions/comments. Below we provide a point-by-point response to individual comment (Reviewer comments and suggestions are in italics, responses and revisions are in plain font; revised parts in responses are marked with red color; page numbers refer to the modified AMTD version).

Comments and suggestions:

Overall Comments. In the work submitted, Li et al. presented the design, construction, and validation of a dynamic chamber system, which can be used to measure uptake coefficient on bulk solid-phase sample. Also, author have shown a relatively good agreement between flow tube, reference, and this study. The technique they developed is very important, and they also carried out tests for operational parameters and validation experiments very comprehensively. The paper is also well-written, and I recommend the manuscript to be published after corrections.

Responses and Revisions:

Thanks for the positive comments and feedback from the reviewer.

Comments and suggestions:

Specific Comments. Page 3 line 25-30: The detailed calculation for uptake coefficient has shown here. The wall-loss effect on the uptake coefficient determination is supposed to discussed in detail. Also, wall-lost correction is necessary to described in 2.1.1. section.

Responses and Revisions:

Thanks for the comments.

Following the reviewer's suggestion, we have added some detailed discussions in the revised manuscript (page 4, line 1-6), as shown below:

"…where C_{ref} (in molecules m^{-3}) is the gas reactant concentration measured at the outlet of a blank chamber prior to the uptake experiment. Since our chamber system had a dynamic flow-through feature, a constant rate of wall loss (once existed) was observed, i.e., the ratio of C_{ref} to C_{in} showed a fixed value during our uptake experiments (see Fig. 3). Thus, using C_{ref} (instead of C_{in}) for flux calculation already accounted for gas losses on chamber walls. Before each gas uptake experiment, C_{ref} was determined mimicking the chamber conditions (i.e., gas flow rate, gas mixing state,

temperature, pressure and RH, and the speed of the mixing fan) of the following uptake experiments."

Comments and suggestions:

Specific Comments. As author explained why outlet position C is used to represent the average concentration due to existence of vertical concentration gradient inside the chamber. However, the smaller horizontal concentration gradient is observed in Fig. 4 and Fig. S2 due to mixing fan. If another mixing fan is placed at both sides of chamber or buffer flask for completing mixing, the vertical concentration gradient might be minimized.

Responses and Revisions:

Thanks for the comments.

As the reviewer pointed out, the smaller horizontal concentration gradient observed in Fig. 4 and Fig. S2 should be due to the incomplete mixing. And vertical concentration gradient can also be minimized by adding a mixing fan at the other side of the chamber (close to the buffer flask on the chamber bottom). However, the related modification/improvement is changeling. The motor used to drive the fan needs to be fixed in a proper way on the bottom side of the chamber, which seems not easy for our current chamber setup. An alternative way may be adding another fan on the lid of the chamber or increasing the speed of the installed fan.

Comments and suggestions:

Specific Comments. Surface morphology of KI coating sample on Vt have shown no significant effects on the deposition velocity. If possible, different preparation on KI sample is better to use optical microscope or SEM/TEM to characterize their morphology.

Responses and Revisions:

Thanks for the suggestion.

As the reviewer suggested, we have added some photos showing the different surface morphologies of the KI coatings prepared via different procedures. Due to the complexity of the coating samples, it is difficult to characterize their morphology by optical microscope or SEM/TEM. The photos are therefore made by a mobile phone camera. The related modifications in the revised manuscript (page 14, line 17-19, and page 15 line 1-5) are shown below:

"… Figure 5 displays the four types of surface phase-state/morphology of the prepared KI coatings. Apparently, different preparation procedures generated distinct surface states/morphologies, especially among Type I, II/III and IV. Figure 6 shows the calculated V_t corresponding to these coating types. …

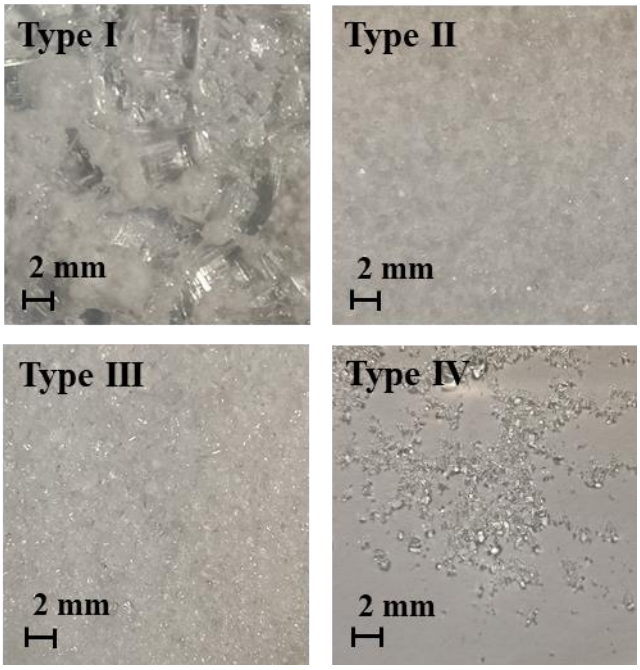

Figure 5. Characteristic morphologies of coated KI (top view) observed by a mobile phone camera. Type I: KI film; Type II: KI grain pre-humidified in a 50% RH N_2 environment for 30 min; Type III: KI grain pre-humidified in a 73% RH N_2 environment for 30 min; Type IV: saturated KI solution with deposited KI grains which cannot be further dissolved. Note that Type IV has a smooth liquid surface."

Comments and suggestions:

Specific Comments. Regarding to Fig. 7, there is a clear boundary for mass transport and surface reaction. Could author explain how to define "surface-reaction-limited", "transition regions", and "transport-limited region"

Responses and Revisions:

Thanks for the comments.

In our manuscript, Fig. 7 (i.e., Fig. 8 in the revised manuscript) is used to give a schematic overview on how an overall uptake is influenced by mass transport (R_t) and reactions on sample surfaces (R_s). For a multiphase reaction (i.e., uptake process), normally a gas reactant first needs

to be transported to the vicinity of a sample (solid or liquid phase), and then collides with the sample surface to trigger certain reactions. If a surface reaction has an extremely low rate (indicative of a very small γ, $R_t << R_s$), the overall uptake process is determined by the surface reaction (surface-reaction-limited region). On the other hand, if transport takes a very long time ($R_t >> R_s$), the overall uptake will be limited by the transportation (transport-limited region). If these two processes have similar rates, both will play a critical role in determining the overall uptake (transition region). In Fig. 8, we artificially define the case when $R_t/R_s < 0.1$ (i.e., one order of magnitude lower) as the surface-reaction-limited region ($R_t << R_s$) and the case when $R_t/R_s > 10$ (i.e., one order of magnitude higher) as transport-limited region ($R_t >> R_s$). And the case in between is defined as the transition region, where R_t is comparable to R_s.

We have added some explanations in the revised manuscript (page 17, Fig. 8 caption and page 18 line 11-17), as shown below:

“

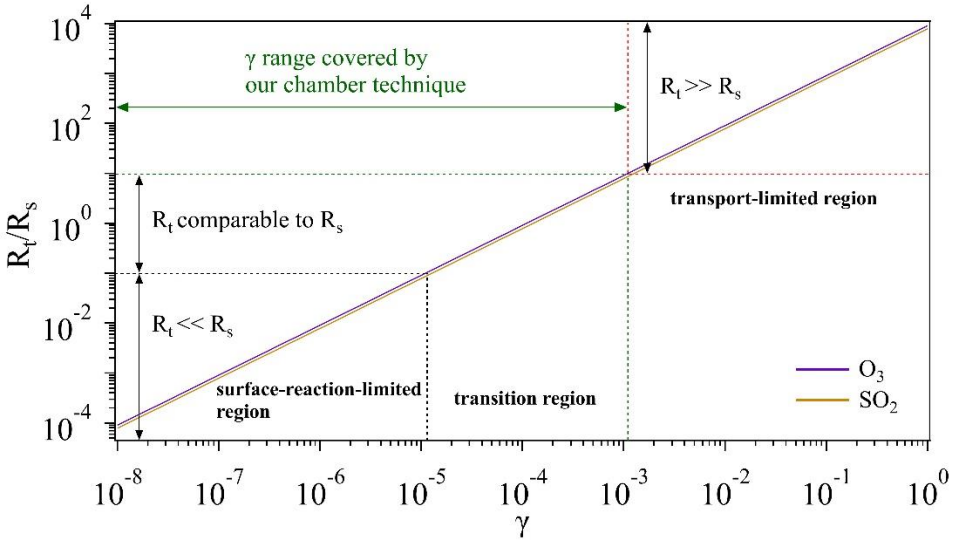

Figure 8. Schematic of different regions for O_3 and SO_2 uptake. Note that we artificially define the case when $R_t/R_s < 0.1$ (i.e., one order of magnitude lower) as the surface-reaction-limited region ($R_t << R_s$) and the case when $R_t/R_s > 10$ (i.e., one order of magnitude higher) as transport-limited region ($R_t >> R_s$). And the case in between is defined as the transition region, where R_t is comparable to R_s. The transport resistance R_t is calculated based on the measured average V_t (Sect. 3.1.3). Calculations for the surface resistance R_s are referred to conditions of room temperature (296 K) and 1 atm.

4 Conclusions

… The chamber results agree well with those from the flow tube method and the literature data.

Figure 8 gives a schematic overview on how an overall uptake is influenced by mass transport (R_t) and reactions on sample surfaces (R_s). For a multiphase reaction (i.e., uptake process), normally a gas reactant first needs to be transported to the vicinity of a sample (solid or liquid phase), and then collides with the sample surface to trigger certain reactions. If a surface reaction has an extremely low rate (indicative of a very small γ, $R_t << R_s$), the overall uptake process is determined by the surface reaction (surface-reaction-limited region). On the other hand, if transport takes a very long time ($R_t >> R_s$), the overall uptake will be limited by the transportation (transport-limited region). If these two processes have similar rates, both will play a critical role in determining the overall uptake (transition region). Given the gas uptake includes both mass transport and surface reaction, its limiting step can be changing as a function of γ. …"